

The Markovian metamorphosis of a simple turbulent cascade model

Jochen Cleve^{1,2} and Martin Greiner^{1,2}

¹*Institut für Theoretische Physik, Technische Universität, D-01062 Dresden, Germany*

²*Max-Planck-Institut für Physik komplexer Systeme, Nöthnitzer Str. 38, D-01187 Dresden, Germany*
(20.03.2000)

Markovian properties of a discrete random multiplicative cascade model of log-normal type are discussed. After taking small-scale resummation and breaking of the ultrametric hierarchy into account, qualitative agreement with Kramers-Moyal coefficients, recently deduced from a fully developed turbulent flow, is achieved.

PACS: 47.27.Eq, 02.50.Ga, 05.40.+j

KEYWORDS: fully developed turbulence, random multiplicative branching process, Markov process.

CORRESPONDING AUTHOR:

Martin Greiner
Max-Planck-Institut für Physik komplexer Systeme
Nöthnitzer Str. 38
D-01187 Dresden, Germany
tel.: 49-351-871-1218
fax: 49-351-871-1199
email: greiner @ mpipks-dresden.mpg.de

Phenomenological modelling of the energy cascade in fully developed turbulence has a long tradition [1,2]. As representatives of the multifractal approach random multiplicative branching processes [3–5] mimic the redistribution of energy flux from the large, integral length scale L down to the small, dissipative scale η and focus on the scaling aspect of the surrogate energy dissipation field, extracted from measured velocity time series. In a particular simple model version, which is only one-dimensional and binary discrete, a domain of length $r_j = L/2^j$ is split into two subdomains of equal length r_{j+1} and the energy flux density $\varepsilon(r_j)$ of the parent domain is non-uniformly redistributed by assigning a left/right multiplicative weight $q_{\mathcal{L}/\mathcal{R}}$ to the left/right subdomain: $\varepsilon_{\mathcal{L}}(r_{j+1}) = q_{\mathcal{L}}\varepsilon(r_j)$, $\varepsilon_{\mathcal{R}}(r_{j+1}) = q_{\mathcal{R}}\varepsilon(r_j)$. The multiplicative weights are drawn from a scale-independent symmetric probabilistic splitting function $p(q_{\mathcal{L}}, q_{\mathcal{R}}) = p(q_{\mathcal{R}}, q_{\mathcal{L}})$, are $\langle q_{\mathcal{L}} \rangle = \langle q_{\mathcal{R}} \rangle = 1$ on average and are completely uncorrelated to multiplicative weights from all other branchings differing in scale and position. At an intermediate length scale $\eta \leq r_j \leq L$, corresponding to j cascade steps, the local bare field density $\varepsilon(r_j) = q_1 q_2 \cdots q_j$ is a product of j independent multiplicative weights, where $\varepsilon(r_0) = 1$ has been chosen for simplicity. Upon taking the logarithm, the product turns into a summation over independent and identically distributed random variables:

$$\ln \varepsilon(r_j) = \ln q_1 + \ln q_2 + \dots + \ln q_j . \quad (1)$$

Introducing $y_j = y(l_j) = \ln \varepsilon(r_j) - \langle \ln \varepsilon(r_j) \rangle$ as new field variable and $l_j = \ln(L/r_j) = j \ln 2$ as a logarithmic scale, it is straightforward to derive

$$\frac{\Delta y}{\Delta l} = \frac{y_{j+1} - y_j}{l_{j+1} - l_j} = \frac{1}{\ln 2} (\ln q_{j+1} - \langle \ln q \rangle) = \sqrt{\frac{\langle \ln^2 q \rangle - \langle \ln q \rangle^2}{2 \ln 2}} \xi_{j+1} \quad (2)$$

from (1) for parent/daughter field variables. The last step, leading to the stationary Gaussian-white noise “random force” ξ_j with normalisation $\langle \xi_j \xi_{j'} \rangle = \frac{2}{\ln 2} \delta_{jj'}$ [6], only holds for a splitting function $p(q_{\mathcal{L}}, q_{\mathcal{R}}) = p(q_{\mathcal{L}})p(q_{\mathcal{R}})$ of log-normal type, where

$$p(q) = \frac{1}{\sqrt{2\pi\sigma q}} \exp\left(-\frac{1}{2\sigma^2} \left(\ln q + \frac{\sigma^2}{2}\right)^2\right) . \quad (3)$$

The Langevin equation (2) represents a discrete Markov process, evolving from large to small scales with zero drift term $D^{(1)} = 0$ and constant diffusion term $D^{(2)} = (\langle \ln^2 q \rangle - \langle \ln q \rangle^2)/2 \ln 2$.

In several ways this thinking seemingly contradicts the results deduced from a large-Reynolds number helium jet experiment [7,8]: from the coarse-grained one-dimensional surrogate energy dissipation field

$$\bar{\varepsilon}(x, r) = \frac{1}{r} \int_{x-\frac{r}{2}}^{x+\frac{r}{2}} \varepsilon(x', \eta) dx' , \quad (4)$$

entering into the transformed variable

$$\bar{y}(x, l) = \ln \bar{\varepsilon}(x, r) - \langle \ln \bar{\varepsilon}(x, r) \rangle , \quad (5)$$

the Kramers-Moyal coefficients

$$D^{(n)}(\bar{y}(l)) = \lim_{\Delta l \rightarrow 0} \frac{1}{n! \Delta l} \int [\bar{y}(l + \Delta l) - \bar{y}(l)]^n p(\bar{y}(l + \Delta l) | \bar{y}(l)) d\bar{y}(l + \Delta l) \quad (6)$$

have been determined to yield

$$\begin{aligned} D^{(1)}(\bar{y}) &= \gamma \bar{y} & (\gamma \approx 0.21) \\ D^{(2)}(\bar{y}) &= D & (D \approx 0.03) \\ D^{(n \geq 3)}(\bar{y}) &\approx 0 . \end{aligned} \quad (7)$$

This outcome suggests that the energy cascade in fully developed turbulence can be described by a scale-continuous Markovian Ornstein-Uhlenbeck process, which differs from the discrete random multiplicative branching picture in two ways: scale-continuous evolution with a linear drift and constant diffusion term as opposed to a scale-discrete evolution with a zero drift and constant diffusion term. – However, the comparison between these two, apparently contradicting pictures is not well taken and is not as straightforward as anticipated. So far it has been like comparing a caterpillar with a butterfly. Now, we will initiate the metamorphosis in two steps.

Step one has to do with the distinction between a bare and a dressed field [9]. Since fully developed turbulence is a three-dimensional process, the redistribution of energy flux from larger to smaller scales should be conserved in three dimensions, as long as the dissipative scale η is not reached. Of course this does not hold once the process is looked at in only one dimension, which is done in one-point time-series measurements of one component of the velocity field and from which the one-dimensional surrogate energy dissipation field is extracted. For the simple binary discrete random multiplicative branching process this implies that the splitting function $p(q_L, q_R) \approx p(q_L)p(q_R)$ more or less factorises, where $p(q)$ should be a positively skewed distribution limited to the support $0 \leq q \leq q_{\max}$ with $q_{\max} \approx 2^3$ [10]. In this respect, the log-normal distribution (3) with the realistic parameter $\sigma = 0.42$, reproducing observed lowest-order scaling exponents $\langle \varepsilon^n(r_j) \rangle \sim (L/r_j)^{\tau(n)}$ and observed multiplier distributions, represents a fair candidate. With a factorised splitting function, where $\langle q_L + q_R \rangle = 2$ only holds on average, we have to distinguish between the bare field (1), which is evolved from the large scale L down to the intermediate scale r_j , and the dressed field

$$\bar{\varepsilon}(r_j) = \varepsilon(r_j)(1 + \Delta(r_j)), \quad (8)$$

which has been evolved from L all the way down to the dissipative scale η and then again resummed up to the intermediate scale r_j . The two fields differ by a small-scale resummation factor $(1 + \Delta(r_j))$, which is equal to one only on average. As the experimental analysis (4) corresponds to the dressed field, we also need to employ the dressed field for the random multiplicative branching process, in order to make a fairer comparison between model and data results.

For a truly fair comparison between model and data results we have to call for an additional, second step: since the binary discrete random multiplicative branching process is organised hierarchically in one-dimensional space, the underlying ultrametric does not allow for spatially homogeneous observables right away. This has been noted only recently [10–12] and a simple scheme has been suggested, breaking the ultrametric hierarchy and restoring spatial homogeneity. It builds a long chain of independent cascade field realisations, each of length L , randomly places the observational interval of length $\eta \leq r \leq L$ within this chain and samples over these random placings.

These two steps have been decisive for the correct interpretation [10,12] of the observed multiplier phenomenology [13,14]: the small-scale resummation of step one explains the scale-independent multiplier distributions as fixed-point distributions and step two is in charge for producing the correct correlations between multipliers. – Since the Kramers-Moyal coefficients (6) can be understood as moments of logarithmic multipliers, defined for an infinitesimal scale step, we might already begin to speculate here that steps one and two might also be in charge for turning the caterpillar (2) into the butterfly (7).

We will now test this speculation by numerical simulation of the binary discrete random multiplicative branching process with the factorised splitting function (3) of log-normal type ($\sigma = 0.42$). A chain of $N_L = 10^6$ independent cascade realisations is constructed, where each realisation has been obtained after $J = 10$ binary cascade steps; consequently the length of the total chain amounts to $10^6 L = 1.28 \cdot 10^9 \eta$.

At first we test the Markov property in general. The conditional probability distributions $p(\bar{y}(l_2)|\bar{y}(l_1))$ with centred intervals $l_2 > l_1$ is sampled over $e^{l_1} N_L$ random placings within the long chain of cascade realisations. It is found that these conditional probability distributions fulfill the Chapman-Kolmogorov equation $p(\bar{y}(l_3)|\bar{y}(l_1)) = \int p(\bar{y}(l_3)|\bar{y}(l_2))p(\bar{y}(l_2)|\bar{y}(l_1))d\bar{y}(l_2)$ close to perfectly in the scale range $\eta \ll l \leq L$. This is a necessary and almost sufficient validation for this branching process to appear Markovian [6].

Without any loss of generality the Kramers-Moyal coefficients (6) are only calculated at binary scales r_j , but again sampled over randomly chosen x -values within the long cascade chain. Convergence is tested by letting the positive integer number $m \rightarrow 1$ in the centred daughter interval of length $r_j - \Delta r_j = r_j - 2m\eta$. Good convergence is achieved for $0 \leq j \leq 5$, i.e. the upper part of the cascade inertial range, whereas for $6 \leq j \leq J = 10$ convergence has been found to be unsatisfactory since $\eta \ll r_j$ is no longer fulfilled. Consequently, in the following we will only show results for the former scale range. – The first Kramers-Moyal coefficient $D^{(1)}(\bar{y}, l)$ is illustrated in Fig. 1a at binary scales $j = 1, 3, 5$. It is not constant zero anymore; now it is linear in $\bar{y}(l_j)$. Fitting the parametrisation $D^{(1)}(\bar{y}, l) = \gamma_0(l) + \gamma(l)\bar{y}$ yields $\gamma_0(l) = 0$ within simulation error bars and a positive, slightly scale-dependent drift coefficient $\gamma(l)$ with values listed in Tab. 1a. The latter decreases from a value 0.19 at $L = 2^9 \eta$ to a value 0.08 at $r_5 = 2^5 \eta$ and agrees with the experimentally deduced value (7) within a factor of 1.1-2.5. The second Kramers-Moyal coefficient $D^{(2)}(\bar{y}, l)$, depicted in Fig. 1b, turns out to be almost constant and almost scale-independent; fitted values of the parametrisation $D^{(2)}(\bar{y}, l) = D(l) + d_1(l)\bar{y}$ can be found in Tab. 1a. Compared with $D = 0.127$ of the caterpillar thinking (2) it is reduced by about a factor of 3, but is still about a factor of 1.4 above the experimentally given result (7). Also in qualitative agreement with the experimental results, higher-order Kramers-Moyal coefficients are close to zero: $D^{(3)}(\bar{y}, l)$ and $D^{(4)}(\bar{y}, l)$ are of the order 10^{-3} and 10^{-4} , respectively. Here we might evoke Pawulas theorem [6] to conclude that, after taking steps one and two into account, the binary discrete random multiplicative branching process of log-normal type appears as a scale-continuous Markovian Ornstein-Uhlenbeck process with Kramers-Moyal coefficients

$$\begin{aligned}
D^{(1)}(\bar{y}) &= \gamma(l)\bar{y} & (0.2 \geq \gamma(l) \geq 0.1) \\
D^{(2)}(\bar{y}) &= D & (D \approx 0.04) \\
D^{(n \geq 3)}(\bar{y}) &\approx 0.
\end{aligned} \tag{9}$$

This result is in nice qualitative agreement with the experimental observation (7).

The result (9) has been obtained by taking both steps, one and two, of the metamorphosis into account. Step one with its small-scale resummation is definitely responsible for the transition from the scale-discrete evolution of the bare field to the scale-continuous Markov description for the dressed field. What are then the implications of step two, i.e. the breaking of the ultrametric cascade hierarchy to restore spatial homogeneity? In order to clarify this point, we restrict the sampling of the Kramers-Moyal coefficients only to the hierarchical positions $x_m = (m+0.5)r_j$ with integer $0 \leq m < 2^j \cdot N_L$ within the long chain of cascade configurations. For these positions, the integration interval of length r_j , entering into (4), perfectly matches an intermediate interval of the bare cascade evolution. Results for the first and second Kramers-Moyal coefficients are listed in Tab. 1b. The first coefficient, which we now denote with a tilde, is again found to be of the form $\tilde{D}^{(1)}(\bar{y}, l) = \tilde{\gamma}(l)\bar{y}$. Note however, that the drift coefficient $\tilde{\gamma}$ is negative and that its modulus is about a factor of 3-7 less when compared with γ . This demonstrates that small-scale resummation alone already introduces a weak linear drift term, but breaking of the ultrametric hierarchy is very necessary to change its sign and to bring it to the correct order of magnitude. Also the second Kramers-Moyal coefficient $\tilde{D}^{(2)}(\bar{y}, l) = \tilde{D}(l) + \tilde{d}_1(l)\bar{y}$ is affected by leaving out step two, but only weakly: again it shows a small scale-dependence, is almost constant for a given scale and, once compared with $D(l)$, is reduced by about a factor of 1.2-1.7. Note also, that it is mainly small-scale resummation, which drives the diffusion coefficient away from the caterpillar thinking (2) with $D = 0.127$.

We conclude: small-scale resummation and breaking of the ultrametric hierarchy initiate the Markovian metamorphosis of a discrete random multiplicative branching process as they turn the caterpillar, a discrete, Gaussian white-noise evolution in scale, into a butterfly, that is an effective scale-continuous Ornstein-Uhlenbeck description, the latter being in qualitative agreement with the experimental observations. At least on a qualitative level, there is no conflict between the experimentally observed energy cascade in fully developed turbulence and random multiplicative branching processes; this statement is further supported by recent work on multiplier distributions [10,12,15]. – Several points have to be considered in order to possibly achieve an even better quantitative agreement between such model results and experimental observations: sensitivity on the generator of random multiplicative branching processes, i.e. on scale-discrete or scale-continuous implementations and on the choice of splitting function, as well as on finite-size, large-scale and dissipative effects; work in these directions is in progress [16]. Also data results for larger Reynolds numbers would be highly appreciated.

-
- [1] U. Frisch, *Turbulence* (Cambridge University Press, Cambridge, 1995).
- [2] T. Bohr, M. Jensen, G. Paladin and A. Vulpiani, *Dynamical Systems Approach to Turbulence* (Cambridge University Press, Cambridge, 1998).
- [3] E.A. Novikov, Appl. Math. Mech. **35**, 231 (1971); Phys. Fluids **A2**, 814 (1990).
- [4] B. Mandelbrot, J. Fluid Mech. **62**, 331 (1974).
- [5] C. Meneveau and K.R. Sreenivasan, J. Fluid Mech. **224**, 429 (1991).
- [6] H. Risken, *The Fokker-Planck Equation* (Springer, Berlin, 1989).
- [7] A. Naert, R. Friedrich and J. Peinke, Phys. Rev. **E56**, 6719 (1997).
- [8] P. Marcq and A. Naert, Physica **D134**, 368 (1998).
- [9] D. Schertzer and S. Lovejoy, J. Geophys. Res. **92**, 9693 (1987).
- [10] B. Jouault, M. Greiner and P. Lipa, Physica **D136**, 125 (2000).
- [11] M. Greiner, J. Gieseemann, and P. Lipa, Phys. Rev. **E56**, 4263 (1997).
- [12] B. Jouault, P. Lipa and M. Greiner, Phys. Rev. **E59**, 2451 (1999).
- [13] K.R. Sreenivasan and G. Stolovitzky, J. Stat. Phys. **78**, 311 (1995).
- [14] G. Pedrizzetti, E.A. Novikov and A.A. Praskovskiy, Phys. Rev. **E53**, 475 (1996).
- [15] B. Jouault, J. Schmiegel and M. Greiner, *chao-dyn/9909033*.
- [16] J. Cleve and M. Greiner, in preparation.

j	(a)			(b)		
	γ	D	d_1	$\tilde{\gamma}$	\tilde{D}	\tilde{d}_1
0	0.154	0.042	-0.004	-0.178	0.036	0.004
1	0.193	0.042	-0.004	-0.077	0.034	0.002
2	0.163	0.040	-0.003	-0.052	0.031	0.001
3	0.133	0.040	-0.002	-0.034	0.029	0.001
4	0.105	0.040	-0.002	-0.021	0.027	0.001
5	0.084	0.043	-0.002	-0.012	0.025	0.001

TABLE I. First and second Kramers-Moyal coefficients, $D^{(1)}(\bar{y}, l_j) = \gamma(l_j)\bar{y}$ and $D^{(2)}(\bar{y}, l_j) = D(l_j) + d_1(l_j)\bar{y}$, after small-scale resummation and (a) with / (b) without breaking of the ultrametric hierarchy.

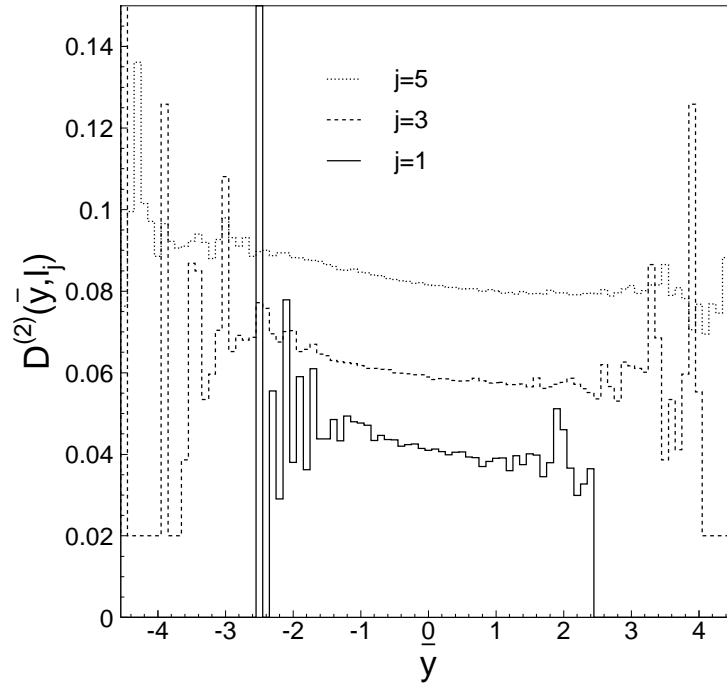
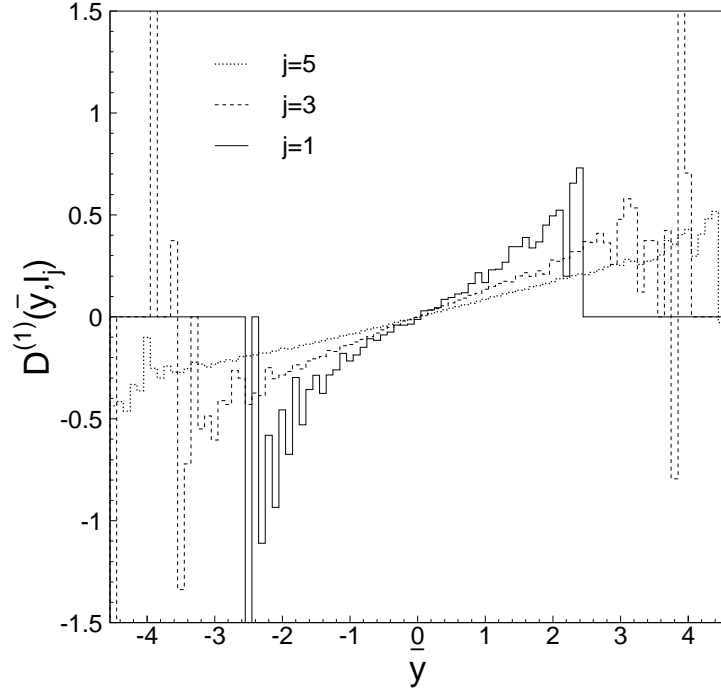


FIG. 1. First (a) and second (b) Kramers-Moyal coefficients, obtained after small-scale resummation and breaking of the ultrametric hierarchy. The $D^{(2)}$ -values for $j = 3$ and 5 have been artificially shifted by 0.02 and 0.04 , respectively.